

Energy Band Engineering of Periodic Scatterers by Quasi-1D Confinement

J. I. Kim*

*Departamento de Física, Instituto de Ciências Ambientais, Químicas e Farmacêuticas
Universidade Federal de São Paulo, Rua São Nicolau 210, 09913-030, Diadema, SP, Brazil.*

A mechanism to modify the energy band structure is proposed by considering a chain of periodic scatterers forming a linear lattice around which an external cylindrical trapping potential is applied along the chain axis. When this trapping (confining) potential is tight enough, it may modify the bound and scattering states of the lattice potential, whose three-dimensional nature around each scattering center is fully taken into account and not resorting to zero-range pseudo-potentials. Since these states contribute to the formation of the energy bands, such bands could thereby be continuously tuned by manipulating the confinement without the need to change the lattice potential. In particular, such dimensionality reduction by quantum confinement can close band gaps either at the center or at the edge of the momentum k -space.

I. INTRODUCTION

Some physical properties of a material generally depend on its electronic band structure, particularly, whether it behaves as a (band) insulator, a semiconductor or a metal [1]. In this regard, rarely can one and the same material be freely driven to become, e.g., either an insulator in one situation or a metal in another, due to the constraint imposed, for example, by the fixed crystal lattice, which determines much of the energy bands. However, designing a material with tunable band structure but without changing its lattice, on the other hand, would be highly desirable for both basic research and technological applications.

Ultracold atoms and optical traps [2] have allowed the simulation of several physical systems [3–6], including also many-body effects. The single-particle band structure in an optical lattice can then be tuned by changing the laser parameters like its intensity and wave length, or by changing the beams' configuration such as tilting the relative angle between the directions of the counter-propagating beams [7–9] or setting a relative non-zero angle between their polarization axes (the so called lin- θ -lin configuration [6, 10, 11]). Although powerful and very convenient, such band structure tuning techniques with optical lattices amount, however, to changing the lattice structure, i.e. to changing the material itself such as its composition (the laser intensity or detuning driving the trap depth of potential minima), size, periodicity, etc.

Several studies show or predict that the band structure of many different materials or systems can in fact be engineered by effectively changing the lattice structure in one way or another or by applying external fields. For instance, one can use controlled impurity doping (e.g. in one-dimensional gold atomic wires [12]), chemical functionalization (e.g. hydrogenating graphene to obtain graphane [13]), mechanical straining (e.g. in two-dimensional graphene monoxide [14]), mechanical deformation (e.g. radial deformation of carbon nan-

otubes [15]), electrically gating bilayer graphene [16–18] or cutting nanoribbons into different widths [19–21]. This latter case is of particular interest here, as it involves geometric quantum confinement, which occurs also in some quantum dot lattices for mesoscopic electrons, in which external walls confine the (otherwise free) internal motion of the particle within the dots and one could also observe related effects on the system energy profile by subjecting them to external electromagnetic fields [22–24].

Geometric quantum confinement is also applied here by analysing a one-dimensional (1D) model [25, 26] akin to ultracold atoms in a 1D optical lattice. Rather than manipulating the lattice potential V_{latt} itself, the band structure is then engineered with an external confining potential U with waveguide-like cylindrical symmetry around the 1D chain of scatterers of V_{latt} . By quasi-1D is meant that one accounts locally for the physical 3D nature of both U and V_{latt} around each lattice site as is described in Sec. II. The main idea stems from previous seminal results in the context of two-body cold atomic collisions in low dimensionality [26–29] demonstrating, first in the s -wave [27] and then in the p -wave approximations [29], that the scattering properties of a single scatterer can be strongly modified when it is placed in a tight atom waveguide. Here this low dimensional physics is generalized to a periodic chain of scatterers and to include simultaneously both the s - and p -scattering waves, thus complementing Ref. [30] without, however, using pure 1D zero-range pseudo-potentials and explicitly revealing how the 1D effective parameters depend on the physical 3D ones, specially on the length scale of the confining potential U . For this purpose, it suffices to apply the analytical techniques developed in Refs. [31–33], although more complete treatments [34–36] could also be used as well. As a result, the band structure substantially changes driven by the confinement, with some gaps vanishing if the so-called dual confinement-induced resonance (CIR) is reached [32, 33], whereby the effective quasi-1D scattering is totally suppressed.

After detailing the present model in Sec. II, its solution around a single lattice site is discussed in Sec. III and extended to the whole lattice in Sec. IV, where the energy bands are calculated as a function of the confining

* kim@unifesp.br

potential length scale. In Sec. V, possible experimental realizations are proposed.

II. A QUASI-1D MODEL SYSTEM

We assume an infinitely long linear lattice, with lattice constant a , and oriented along the z -axis. The periodic lattice potential then satisfies $V_{latt}(\mathbf{r} + n_3 a \mathbf{e}_3) = V_{latt}(\mathbf{r})$ for $n_3 = 0, \pm 1, \pm 2, \dots$, where $\mathbf{r} = (x, y, z)$ is the position vector from the site placed at the origin (zeroth site) and \mathbf{e}_3 is the unit vector along the z -axis. Usually $V_{latt} < 0$, i.e. attractive. In the most symmetric configuration, the confining potential may be given by a cylindrically symmetric function $U(\rho)$, where $\rho = (x^2 + y^2)^{1/2}$ is the distance from the lattice symmetry z -axis. In general, $U(\rho)$ is taken to be zero at $\rho = 0$ and to grow positive as ρ increases. The Hamiltonian H for a spinless particle of mass m is then

$$H = -\frac{\hbar^2}{2m} \nabla^2 + U(\rho) + V_{latt}(\mathbf{r}). \quad (1)$$

Two symmetries can be identified here, an external one brought about by the confinement and the local one associated to each lattice site. It is by exploring the interplay between them that a band structure mechanism is proposed.

Under a few proof-of-concept approximations, an analytical solution can be readily obtained. Although many functions $U(\rho)$ and other geometries for the confinement are possible (e.g. $U_1(x) + U_2(y)$), we adopt here the simplest variant by approximating $U(\rho)$ by a square-well type function, namely, $U(\rho) = 0$ for $\rho < R_U$ and infinite otherwise, R_U being the range of $U(\rho)$. A second important assumption is to approximate $V_{latt}(\mathbf{r})$ around each lattice site by a spherically symmetric potential V , namely

$$V_{latt}(\mathbf{r}) \approx V(r), \quad (2a)$$

for \mathbf{r} around the zeroth site, where $r = |\mathbf{r}| = (x^2 + y^2 + z^2)^{1/2}$, and $V_{latt}(\mathbf{r}) \approx V(|\mathbf{r} - n_3 a \mathbf{e}_3|)$ for \mathbf{r} around the n_3 -th site and so forth, thus implying $R_V \ll a$, where R_V is the range of V . As for the range R_U , we assume

$$R_V \ll R_U \ll a, \quad (2b)$$

i.e. the lattice interaction occurs predominantly at the center of the confinement, which in turn is taken to be very tight relative to the lattice dimension. It should be noted that these restrictions are enough for the present purposes but can be lifted in more involved analytical and numerical calculations.

The solution $\Psi(\mathbf{r})$ to Eq.(1) should obey Bloch's condition, one form of which is $\Psi(\mathbf{r} + n_3 a \mathbf{e}_3) = e^{in_3 a k} \Psi(\mathbf{r})$, for some k . A more convenient form is to shift $\mathbf{r} + n_3 a \mathbf{e}_3 \rightarrow \mathbf{r}$ to get

$$\Psi(\mathbf{r}) = e^{in_3 a k} \Psi(\mathbf{r} - n_3 a \mathbf{e}_3), \quad (3)$$

so that the solution $\Psi(\mathbf{r})$ around any lattice site, say at $n_3 a \mathbf{e}_3$ (i.e. \mathbf{r} around $n_3 a \mathbf{e}_3$), can be expressed in terms of the solution $\Psi(\mathbf{r} - n_3 a \mathbf{e}_3)$ around the origin (i.e. $\mathbf{r} - n_3 a \mathbf{e}_3$ around $\mathbf{0}$). Therefore, one can focus on this latter solution (Sec. III) and then expand it via Bloch's condition above to cover the whole lattice (Sec. IV).

III. LOCAL STATES UNDER CONFINEMENT

In order to find the solution $\Psi(\mathbf{r}) \equiv \Psi_0(\mathbf{r})$ around the site at the origin, we note that from Eq.(2a) the Schrödinger equation for Ψ_0 follows from Eq.(1), namely

$$\left[-\frac{\hbar^2}{2m} \nabla^2 + U(\rho) + V(r) \right] \Psi_0 = E \Psi_0, \quad |z| < a/2, \quad (4)$$

where E is the total energy and where two conflicting symmetries (those of U and V) can be clearly seen. As a first treatment to illustrate the principle, we assume $E \equiv \hbar^2 K^2 / 2m > 0$ and deal with running waves bound only by the lateral confinement ($E < 0$ would correspond to the case of states deeply bound to the lattice sites, although U could raise E towards higher energies if it is tight enough to reach such deep states). It turns out that precisely this Eq.(4) has already been studied in the context of cold atom scattering under confinement (see e.g. Refs. [31–33, 37] directly related to the present technique), in which case V is the atom-atom interaction potential and U is the confining laser optical potential, so that much of the analysis for cold atoms remains valid. However, Bloch's condition introduces important changes, such as a different boundary condition. For this reason and for the sake of completeness, we repeat details of the analysis.

Indeed, let φ_n , for $n = 0, 1, 2, \dots$, be the orthonormalized eigenstates of U regular at $\rho = 0$ with eigenvalues $\hbar^2 q_n^2 / 2m > 0$ and satisfying

$$\left[-\left(\frac{\partial^2}{\partial x^2} + \frac{\partial^2}{\partial y^2} \right) + u \right] \varphi_n = q_n^2 \varphi_n, \quad n = 0, 1, 2, \dots, \quad (5a)$$

where $u \equiv 2m U(\rho) / \hbar^2$. Since $V(r)$ in Eq.(4) does not depend on the azimuthal angle ϕ (that encircling the z -axis) either, one can take both $\varphi_n = \varphi_n(\rho)$ and Ψ_0 as axially symmetric. For example, in the specific case of a square-well U , one obtains Bessel functions J_m

$$\varphi_n(\rho) = \frac{N_n}{\pi^{1/2} R_U} J_0(q_n \rho), \quad (5b)$$

where $N_n \equiv |J_1(r_{n+1})|^{-1}$ and r_{n+1} is the $(n+1)$ -th root of J_0 , with $q_n R_U = r_{n+1}$. A good approximation to q_n is given by Eq.(13b) in [31], namely, $q_n \approx (n + 3/4)\pi / R_U$. Decomposing then Ψ_0 on such type of basis $\{\varphi_n\}$,

$$\Psi_0(\mathbf{r}) = \sum_{n=0}^{\infty} \psi_n(z) \varphi_n(\rho), \quad (6)$$

substituting back into Eq.(4) and using the orthonormality of $\{\varphi_n\}$ gives for each $\psi_n(z)$

$$\left(\frac{d^2}{dz^2} + k_n^2\right) \psi_n = \int dx dy \varphi_n^*(\rho) v(r) \Psi_0(\mathbf{r}), \quad (7)$$

where $k_n^2 \equiv K^2 - q_n^2$ and $v(r) \equiv 2mV(r)/\hbar^2$. A general solution $G_n(z, z')$ to the 1D Green's function equation $G_n''(z, z') + k_n^2 G_n(z, z') = -\delta(z - z')$ is

$$G_n(z, z') = -\xi_{n+} \frac{e^{ik_n|z-z'|}}{2ik_n} - \xi_{n-} \frac{e^{-ik_n|z-z'|}}{2i(-k_n)}, \quad (8)$$

where $\xi_{n+} + \xi_{n-} = 1$. For now, the inward scattering wave ξ_{n-} is also kept (as if to account for an incoming flux from the lateral sites), but later we will be able to discard it based on boundary conditions, notably for $a \rightarrow \infty$. Then ψ_n can be written as

$$\begin{aligned} \psi_n(z) = & A_n e^{ik_n z} + B_n e^{-ik_n z} \\ & - \int d^3 \mathbf{r}' G_n(z, z') \varphi_n^*(\rho') v(r') \Psi_0(\mathbf{r}'), \end{aligned} \quad (9)$$

where the first two terms are homogeneous solutions to the left-hand side (lhs) of Eq.(7), representing forward and backward running waves, respectively. One can now write Eq.(6) as

$$\begin{aligned} \Psi_0(\mathbf{r}) = & \sum_{n=0}^{\infty} (A_n e^{ik_n z} + B_n e^{-ik_n z}) \varphi_n(\rho) \\ & - \sum_{n=0}^{\infty} \int d^3 \mathbf{r}' G_n(z, z') \varphi_n^*(\rho') v(r') \Psi_0(\mathbf{r}') \varphi_n(\rho). \end{aligned} \quad (10)$$

Suppose now for simplicity that only the ground state channel $n = 0$ is open, that is,

$$0 \leq q_0^2 \leq K^2 \leq q_1^2. \quad (11)$$

For $n \geq 1$, k_n is then imaginary, say $k_n = i(q_n^2 - K^2)^{1/2}$, and thus ξ_{n-} must vanish (so that $\xi_{n+} = 1$), otherwise the second term on the right-hand side (rhs) of Eq.(10) for $z \sim a/2$ would be exponentially large as $e^{+a/2R_U}$ (see Eq.(2b)), since $k_n \sim q_n \sim 1/R_U$ or larger and the solution would diverge in the limit $a \rightarrow \infty$ of a single site; besides, if Eq.(10) is to be finite for both $z \sim -a/2$ and $z \sim +a/2$, the A_n and B_n , respectively, must also vanish. We have thus

$$\begin{aligned} \Psi_0(\mathbf{r}) = & (A_0 e^{ik_0 z} + B_0 e^{-ik_0 z}) \varphi_0(\rho) \\ & - \int d^3 \mathbf{r}' G_0(z, z') \varphi_0^*(\rho') v(r') \Psi_0(\mathbf{r}') \varphi_0(\rho) \\ & + \sum_{n=1}^{\infty} \int d^3 \mathbf{r}' \frac{e^{ik_n|z-z'|}}{2ik_n} \varphi_n^*(\rho') v(r') \Psi_0(\mathbf{r}') \varphi_n(\rho), \end{aligned} \quad (12)$$

where we take $k_0 \equiv +\sqrt{K^2 - q_0^2} > 0$.

In order to impose Bloch's condition Eq.(3) (see also Eqs.(34a) and (34b)), we need to know the behaviour of Ψ_0 near the zero-th site boundaries $|z| \sim a/2$. In this

region, z predominates over z' , since z' is limited to the range $R_V \ll a$ in the integrands above. Hence, for $z \sim a/2$, $z - z'$ is positive and thus $|z - z'| = z - z'$, whereas for $z \sim -a/2$, $z - z'$ is negative and thus $|z - z'| = -z + z'$, in other words, $|z - z'| = |z| \mp z'$ if $z \sim \pm a/2$. One notes also that each term of the series for $n \geq 1$ in Eq.(12) becomes exponentially small for $|z| \sim a/2$, scaling as $e^{-a/2R_U}$ or less. As part of the approximations used here, we neglect them. In this way, Eq.(12) becomes for $z \sim \pm a/2$

$$\begin{aligned} \Psi_0(\mathbf{r}) \approx & (A_0 e^{ik_0 z} + B_0 e^{-ik_0 z}) \varphi_0(\rho) \\ & + \left(\xi_{0+} f_{0+}^{\pm} e^{ik_0|z|} + \xi_{0-} f_{0-}^{\pm} e^{-ik_0|z|} \right) \varphi_0(\rho), \end{aligned} \quad (13a)$$

the scattering amplitudes f_{0+}^{\pm} and f_{0-}^{\pm} being defined as

$$\begin{aligned} f_{0+}^{\pm} & \equiv \frac{1}{2ik_0} \int d^3 \mathbf{r}' \left[e^{\pm ik_0 z'} \varphi_0(\rho') \right]^* v(r') \Psi_0(\mathbf{r}'), \\ f_{0-}^{\pm} & \equiv \frac{1}{2i(-k_0)} \int d^3 \mathbf{r}' \left[e^{\pm i(-k_0)z'} \varphi_0(\rho') \right]^* v(r') \Psi_0(\mathbf{r}'), \end{aligned} \quad (13b)$$

the upper (+) sign referring to $z \sim +a/2$ and the upper (−) sign referring to $z \sim -a/2$.

These amplitudes f_{0+}^{\pm} and f_{0-}^{\pm} depend on the behaviour of Ψ_0 in the region R_V close to the origin, where the spherical symmetry of V prevails instead of the cylindrical one close to the borders $|z| \sim a/2$. It is more convenient then to replace the cylindrical basis vector $e^{\pm ik_0 z} \varphi_0(\rho)$ by a spherical basis, namely by trying

$$e^{ik_0 z} \varphi_0(\rho) = \sum_{l=0}^{\infty} [i^l (2l+1) \alpha_{0l}] j_l(Kr) P_l(\cos \theta), \quad (14a)$$

for some constants α_{0l} , where θ is the polar angle, j_l and P_l are spherical Bessel functions and Legendre polynomials, respectively, and the coordinate transformation is $z = r \cos \theta$ and $\rho = r \sin \theta$. If U in Eq.(5a) is of the square-well type, α_{0l} can be calculated exactly (see Eqs.(13) and (17) in [31] and Eq.(11.3.49) in [38], Vol.II, §11.3)

$$\alpha_{0l} = \frac{1}{\pi^{1/2} d_U} P_l(k_0/K), \quad (14b)$$

where $d_U \equiv R_U/N_0$. When inserting Eq.(14a) into Eqs.(13b), we use $-z = r \cos(\pi - \theta)$ and the property $P_l(\cos(\pi - \theta)) = (-1)^l P_l(\cos \theta)$; in addition, we separate the l -summation into even $l = 0, 2, 4, \dots$ and odd $l = 1, 3, 5, \dots$ groups, so that Eq.(13b) becomes

$$f_{0+}^{\pm} = \sum_{l=\text{even}}^{\infty} \frac{4\pi(2l+1)\alpha_{0l}^*}{2ik_0} T_l \pm \sum_{l=\text{odd}}^{\infty} \frac{4\pi(2l+1)\alpha_{0l}^*}{2ik_0} T_l, \quad (15a)$$

$$f_{0-}^{\pm} = - \sum_{l=\text{even}}^{\infty} \frac{4\pi(2l+1)\alpha_{0l}^*}{2ik_0} T_l \pm \sum_{l=\text{odd}}^{\infty} \frac{4\pi(2l+1)\alpha_{0l}^*}{2ik_0} T_l, \quad (15b)$$

where T_l are scattering amplitudes in the spherical basis

$$T_l \equiv \int \frac{d^3 \mathbf{r}'}{i^l 4\pi} [j_l(Kr') P_l(\cos \theta')] v(r') \Psi_0(\mathbf{r}'). \quad (16)$$

For these T_l , one can not use Eq.(13a), but needs Ψ_0 within the range R_V . Following [31–33], the idea is to transform the rhs of the full solution Eq.(12) using spherical coordinates, which will naturally bring about the amplitudes T_l . For this purpose, we note that $r' \sim R_V \ll R_U$ and set $r \ll R_U$ as well, such that Eq.(12) becomes

$$\Psi_0(\mathbf{r}) = \Psi_{0i}(\mathbf{r}) - \int d^3 \mathbf{r}' G_c(\mathbf{r}, \mathbf{r}') v(r') \Psi_0(\mathbf{r}'), \quad (17)$$

where $\Psi_{0i}(\mathbf{r}) \equiv (A_0 e^{ik_0 z} + B_0 e^{-ik_0 z}) \varphi_0(\rho)$ and the axially symmetric Green's function G_c is, for $r, r' \ll R_U$,

$$\begin{aligned} G_c(\mathbf{r}, \mathbf{r}') &= i(\xi_{0+} - \xi_{0-}) \varphi_0^*(\rho') \varphi_0(\rho) \frac{\cos(k_0|z - z'|)}{2k_0} \\ &\quad - \varphi_0^*(\rho') \varphi_0(\rho) \frac{\sin(k_0|z - z'|)}{2k_0} \\ &\quad + \int_{q_1}^{\infty} \frac{q dq}{4\pi} J_0(q\rho') J_0(q\rho) \frac{e^{-\sqrt{q^2 - K^2}|z - z'|}}{\sqrt{q^2 - K^2}}, \end{aligned} \quad (18)$$

where we used $k_n = +i(q_n^2 - K^2)^{1/2}$ for $n \geq 1$ and the third term, originally a discret summation over n , has been replaced by its continuum limit (see Eq.(13b) et seq. in [31]) valid for $r, r' \ll R_U$. Note that Eq.(17) can also be expressed alternatively by formally substituting G_c by a non-axially symmetric Green's function G_u satisfying $[\nabla^2 - u(\rho) + K^2]G_u(\mathbf{r}, \mathbf{r}') = -\delta(\mathbf{r} - \mathbf{r}')$, such that $2\pi G_c = \int d\phi' G_u$ since G_c , v and Ψ_0 do not depend on ϕ' in Eq.(17), where the ϕ' integration can be made to yield the factor 2π . As is discussed in Sec.(IV.B) of [31], for $r, r' \ll R_U$, such that $u(\rho) \approx 0$, G_u should differ from the free-space 3D Green's function $G(\mathbf{r}, \mathbf{r}')$ satisfying $[\nabla^2 + K^2]G(\mathbf{r}, \mathbf{r}') = -\delta(\mathbf{r} - \mathbf{r}')$ by at most a homogeneous term $\Delta_u(\mathbf{r}, \mathbf{r}')$ satisfying $[\nabla^2 + K^2]\Delta_u(\mathbf{r}, \mathbf{r}') = 0$, so that

$$G_c(\mathbf{r}, \mathbf{r}') \approx \int_0^{2\pi} \frac{d\phi'}{2\pi} G(\mathbf{r}, \mathbf{r}') + \Delta_c(\mathbf{r}, \mathbf{r}'), \quad (19)$$

with $\Delta_c(\mathbf{r}, \mathbf{r}') \equiv \int d\phi' \Delta_u(\mathbf{r}, \mathbf{r}')/2\pi$ and where

$$G(\mathbf{r}, \mathbf{r}') \equiv \gamma_+ \frac{e^{iK|\mathbf{r} - \mathbf{r}'|}}{4\pi|\mathbf{r} - \mathbf{r}'|} + \gamma_- \frac{e^{-iK|\mathbf{r} - \mathbf{r}'|}}{4\pi|\mathbf{r} - \mathbf{r}'|} \quad (20)$$

with $\gamma_+ + \gamma_- = 1$. In order to identify $\Delta_c(\mathbf{r}, \mathbf{r}')$ and these γ 's, one expands $G(\mathbf{r}, \mathbf{r}')$ in cylindrical coordinates using (see, e.g. [38], Vol.I, Chap. 7, problem 7.9)

$$\begin{aligned} \frac{e^{iK|\mathbf{r} - \mathbf{r}'|}}{4\pi|\mathbf{r} - \mathbf{r}'|} &= - \sum_{m=0}^{\infty} (2 - \delta_{0,m}) \cos[m(\phi - \phi')] \\ &\quad \times \int_0^{\infty} \frac{q dq}{4\pi} J_m(q\rho) J_m(q\rho') \frac{e^{i\sqrt{K^2 - q^2}|z - z'|}}{i\sqrt{K^2 - q^2}} \end{aligned} \quad (21)$$

with the correct branch $0 \leq \arg \sqrt{K^2 - q^2} < \pi$ and taking the complex conjugate to generate the expansion of $e^{-iK|\mathbf{r} - \mathbf{r}'|}/4\pi|\mathbf{r} - \mathbf{r}'|$. We next substitute these expansions into the rhs of Eq.(19), whose lhs in turn follows from Eq.(18), and compare both sides to get for $r, r' \ll R_U$

$$\gamma_+ = \gamma_- = 1/2, \quad (22a)$$

$$\begin{aligned} \Delta_c(\mathbf{r}, \mathbf{r}') &\approx - \int_0^{p_c} \frac{dp}{4\pi} J_0(q\rho') J_0(q\rho) e^{-p|z - z'|} \\ &\quad + i(\xi_{0+} - \xi_{0-}) \varphi_0^*(\rho') \varphi_0(\rho) \frac{\cos(k_0|z - z'|)}{2k_0}, \end{aligned} \quad (22b)$$

where $q = \sqrt{K^2 + p^2}$ and $p_c \equiv \sqrt{q_1^2 - K^2}$. Here, Eq.(22a) and Eq.(22b) are improvements to Eq.(16a) and Eq.(16b), respectively, of [31] and follows the discussion given in [32, 33]. Physically, Eq.(22a) accounts for an inward particle flux arising from reflections of the outward scattered wave against the boundaries of the confinement. The integral in Δ_c stems from the lower limit q_1 in the q -integration in Eq.(18) and the limit K implicit in the q -integration in Eq.(21), whereas a term involving $\sin(\sqrt{K^2 - q^2}|z - z'|)$ and one involving $\sin(k_0|z - z'|)$ have been neglected, since they are a factor $|z - z'|/R_U \ll 1$ smaller than the first and second terms, respectively, of Eq.(22b). Because of the modulus $|z - z'|$ rather than $z - z'$, Δ_c in Eq.(22b) is not precisely an axially symmetric plane wave (in cylindrical coordinates, with φ_0 being Bessel functions) satisfying the original requirement $[\nabla^2 + K^2]\Delta_c(\mathbf{r}, \mathbf{r}') = 0$, stemming from Δ_u . On the other hand, this modulus plays an important part in causing the decoupling of partial waves l and s for which $l + s$ is odd, as is discussed when deriving Eq.(25) below. In any case, detailed numerical calculations [32, 37] showed satisfactory agreements with such analytical approximations made here. For this reason, this Δ_c will be kept in the following.

The next step to calculate T_l is to replace $G_c(\mathbf{r}, \mathbf{r}')$ in Eq.(17) by the rhs of Eq.(19), using the results Eqs.(20), (22a) and (22b). In this way, one can safely expand the rhs of Eq.(17) in spherical coordinates. For Ψ_{0i} one uses directly Eq.(14a). For G , one needs (see e.g. Eq.(11.3.44) in [38], Vol.II, §11.3)

$$\begin{aligned} \frac{e^{iK|\mathbf{r} - \mathbf{r}'|}}{4\pi|\mathbf{r} - \mathbf{r}'|} &= \quad \quad \quad r' < r \quad (23) \\ &\frac{iK}{4\pi} \sum_{l=0}^{\infty} (2l+1) \times \sum_{m=0}^l \epsilon_m \frac{(l-m)!}{(l+m)!} \cos[m(\phi - \phi')] \\ &\quad \times P_l^m(\cos \theta') P_l^m(\cos \theta) j_l(Kr') [j_l(Kr) + i n_l(Kr)], \end{aligned}$$

where $\epsilon_m = 1$ for $m = 0$ and $\epsilon_m = 2$ otherwise, n_l is the spherical Neumann function and P_l^m is the associated Legendre function. As for Δ_c in Eq.(22b), one rewrites $|z - z'| = z\sigma_{zz'} - z'\sigma_{zz'}$, with $\sigma_{zz'} \equiv \text{sign}(z - z')$; for its second term on the rhs one uses Eq.(14a) twice (for \mathbf{r} and then for \mathbf{r}') and for its first term, on the other hand, one continues Eq.(14a) analytically to the imaginary $k_0 \rightarrow ip$

axis to get (assuming square-well type U)

$$e^{-pz} J_0(q\rho) = \sum_{l=0}^{\infty} i^l (2l+1) P_l(ip/K) j_l(Kr) P_l(\cos\theta), \quad (24)$$

which is then also used twice. We now substitute these results into the rhs of Eq.(19) and cast Eq.(17) as an expansion in the spherical basis $\{j_l P_l\}$ valid for $r \ll R_U$. In doing so, one must carefully track signs such as $(-)^l$, $(-)^s$, $(\sigma_{zz'})^l$ and $(\sigma_{zz'})^s$ and eliminate spurious couplings between even and odd angular momenta arising from Eq.(22b) (see discussion after Eq.(20) in [31]), since $\langle l|U|s\rangle = 0$ if $l+s = \text{odd}$, which then sets $(-)^{l+s} = (\sigma_{zz'})^{l+s} = +1$. As a result, Eq.(17) becomes for $r \ll R_U$

$$\begin{aligned} \Psi_0(\mathbf{r}) \approx & \sum_{l=0}^{\infty} i^l (2l+1) \left[\alpha_l + \gamma_l^{(1)} + i\gamma_l^{(2)} \right] j_l(Kr) P_l(\cos\theta) \\ & + \sum_{l=0}^{\infty} i^l (2l+1) [KT_l] n_l(Kr) P_l(\cos\theta), \end{aligned} \quad (25)$$

where $\alpha_l \equiv [A_0 + (-1)^l B_0] \alpha_{0l}$ and the $\gamma_l^{(m)}$'s are defined by $\gamma_l^{(m)} \equiv \sum_{s[l]} (2s+1) P_{ls}^{(m)} T_s$, with $s[l]$ being a sum over all even (odd) s for a given even (odd) l , and

$$P_{ls}^{(1)} \equiv K \int_0^{p_c/K} dx P_l(ix) P_s(ix), \quad (26a)$$

$$P_{ls}^{(2)} \equiv -(\xi_{0+} - \xi_{0-}) \frac{2\pi}{k_0} \alpha_{0l} \alpha_{0s}. \quad (26b)$$

We now set $R_V \ll r \ll R_U$ and recall that then the above Ψ_0 in Eq.(25) should correspond to a standard well-known spherical scattering solution emanating from V (supposed of short range) and thus having the form (see e.g. [39], §132)

$$\Psi_0(\mathbf{r}) \approx \sum_{l=0}^{\infty} c_l [\cos \delta_l j_l(Kr) - \sin \delta_l n_l(Kr)] P_l(\cos\theta) \quad (27)$$

where δ_l is the physical 3D l -th angular momentum component scattering phase-shift. Comparing with Eq.(25) term by term and then eliminating the c_l 's, one gets for T_l the following matrix equation for $l = 0, 1, 2, \dots$

$$-(K \cot \delta_l) T_l = \alpha_l + \sum_{s[l]} (2s+1) \left[P_{ls}^{(1)} + i P_{ls}^{(2)} \right] T_s \quad (28)$$

which allows us to obtain T_l and $f_{0\pm}^{\pm}$ in Eqs.(15a) and (15b), thus completing the calculation of Eq.(13a). Although higher partial waves could be collected from Eq.(28), in the low energy condition $R_V \ll R_U$, it is usually a good approximation to retain only the leading phase-shifts δ_0 and δ_1 (see also discussion in Sec.V.C

of [31]). Solving then Eq.(28) for T_0 and T_1 , one gets

$$f_{0+}^{\pm} = -\frac{A_0 + B_0}{(\xi_{0+} - \xi_{0-}) + i \cot \delta_{even}} \mp \frac{A_0 - B_0}{(\xi_{0+} - \xi_{0-}) + i \cot \delta_{odd}}, \quad (29a)$$

$$f_{0-}^{\pm} = \frac{A_0 + B_0}{(\xi_{0+} - \xi_{0-}) + i \cot \delta_{even}} \mp \frac{A_0 - B_0}{(\xi_{0+} - \xi_{0-}) + i \cot \delta_{odd}}, \quad (29b)$$

where the 1D phase-shifts δ_{even} and δ_{odd} are defined by

$$\cot \delta_{even} \equiv [(K \cot \delta_0) d_U \quad (30a)$$

$$+ (C^2 - d_U^2 k_0^2)^{1/2}] \frac{k_0 d_U}{2},$$

$$\cot \delta_{odd} \equiv [(K^3 \cot \delta_1) d_U^3 - (C^2 - d_U^2 k_0^2)^{3/2}] \frac{1}{6 k_0 d_U}, \quad (30b)$$

with $C \equiv \sqrt{q_1^2 - q_0^2} d_U^2$.

In solving Eq.(13a), we still need to calculate $\xi_{0\pm}$. In this regard, note that the above solutions for f_{0+}^{\pm} and f_{0-}^{\pm} make more apparent the fact that the poles of f_{0+}^{\pm} and f_{0-}^{\pm} for imaginary $k_0 \equiv i k_{0B}$ are equal, something that was implicit already in Eqs.(15a) and (15b). Such a pole is related to the bound state spectrum (see also discussion in Sec.V.E in [31]), in the sense that the first term on the rhs of Eq.(13a) (the propagating part) becomes negligible relative to the interacting terms in $e^{\pm k_{0B}|z|}$. If one wants then to retain the single site picture of a bound-state-like exponentially decaying tail in the limit $a \rightarrow \infty$, it follows that ξ_{0-} must vanish in order to kill the diverging term $e^{+k_{0B}|z|}$ brought about by f_{0-}^{\pm} . Hence, by virtue of such boundary conditions about bound states in the limit $a \rightarrow \infty$, we set $\xi_{0-} = 0$ and $\xi_{0+} = 1$, such that Eq.(13a) for $|z| \sim a/2$ becomes finally

$$\Psi_0(\mathbf{r}) \approx A_0 \psi_L(z) \varphi_0(\rho) + B_0 \psi_R(z) \varphi_0(\rho), \quad (31a)$$

where $\psi_{L(R)}(z)$ describe a quasi-1D scattering of particles coming from the left (right) and are given by

$$\psi_L(z) \equiv \begin{cases} e^{ik_0 z} + A_r e^{-ik_0 z}, & z \sim -a/2 \\ A_t e^{ik_0 z}, & z \sim +a/2 \end{cases} \quad (31b)$$

$$\psi_R(z) \equiv \begin{cases} A_t e^{-ik_0 z}, & z \sim -a/2 \\ e^{-ik_0 z} + A_r e^{ik_0 z}, & z \sim +a/2 \end{cases} \quad (31c)$$

the quasi-1D scattering amplitudes $A_{t(r)}$ being defined by

$$A_t \equiv 1 - \frac{1}{1 + i \cot \delta_{even}} - \frac{1}{1 + i \cot \delta_{odd}}, \quad (31d)$$

$$A_r \equiv -\frac{1}{1 + i \cot \delta_{even}} + \frac{1}{1 + i \cot \delta_{odd}} \quad (31e)$$

and satisfying the conservation condition

$$|A_t|^2 + |A_r|^2 = 1, \quad (31f)$$

valid for all real δ_{even} and δ_{odd} , as can be verified explicitly. This constitutes the general local solution at the borders of the site at the origin. The constants A_0 and B_0 are determined below from Bloch's condition.

IV. ENERGY BANDS UNDER CONFINEMENT

In order to obtain the solution $\Psi(\mathbf{r})$ valid around all other sites, it is necessary to recall that it must satisfy well known continuity conditions. In our case, due to the way this solution is being constructed, they should be set at the site boundaries. For the site at the origin, for instance, one has at its right boundary at $z = +a/2$

$$\Psi(x, y, a^-/2) = \Psi(x, y, a^+/2), \quad (32a)$$

$$\frac{\partial}{\partial z} \Psi(x, y, a^-/2) = \frac{\partial}{\partial z} \Psi(x, y, a^+/2), \quad (32b)$$

where $a^-/2$ denotes the limit $z \rightarrow +a/2$ from the left and $a^+/2$ denotes this limit from the right. We now use $\Psi_0(\mathbf{r})$ in Bloch's equation Eq.(3) for $n_3 = 0$ (\mathbf{r} around the site at the origin) and for $n_3 = +1$ (\mathbf{r} around the first site to the right), thus

$$\Psi(x, y, z) = \begin{cases} \Psi_0(x, y, z), & |z| < a/2, \\ e^{ika} \Psi_0(x, y, z - a), & |z - a| < a/2. \end{cases} \quad (33)$$

Clearly, the first line should be used on the lhs of Eqs.(32a) and (32b) and the second line on their rhs, so that

$$\Psi_0(x, y, a/2) = e^{ika} \Psi_0(x, y, -a/2), \quad (34a)$$

$$\frac{\partial}{\partial z} \Psi_0(x, y, a/2) = e^{ika} \frac{\partial}{\partial z} \Psi_0(x, y, -a/2). \quad (34b)$$

For the next boundary at $z = +3a/2$, one uses $\Psi(\mathbf{r}) = e^{ika} \Psi_0(\mathbf{r} - a\mathbf{e}_z)$ for the left limit of $z \rightarrow +3a/2$ (i.e. \mathbf{r} around the site at $n_3 = +1$) and $\Psi(\mathbf{r}) = e^{i2ka} \Psi_0(\mathbf{r} - 2a\mathbf{e}_z)$ for the right limit (i.e. \mathbf{r} around the site at $n_3 = +2$); the continuity conditions then turn out to be the same, as it should. In other words, Bloch's condition guarantee the continuity along the whole lattice.

Using now Eq.(31a), it can be seen that Eqs.(34a) and (34b) become an homogeneous system of equations for A_0 and B_0 . This system will have a non-zero solution only if its determinant vanishes, that is,

$$0 = (\psi_{L+} - e^{ika} \psi_{L-}) (\psi'_{R+} - e^{ika} \psi'_{R-}) - (\psi'_{L+} - e^{ika} \psi'_{L-}) (\psi_{R+} - e^{ika} \psi_{R-}), \quad (35)$$

with $\psi_{L(R)\pm} \equiv \psi_{L(R)}(\pm a/2)$, $\psi'_{L(R)\pm} \equiv \psi'_{L(R)}(\pm a/2)$. Multiplying this equation by e^{-ika} and using Eqs.(31b) and (31c), one obtains after a tedious but straightforward algebra

$$\frac{A_t^2 - A_r^2}{2A_t} e^{ik_0 a} + \frac{1}{2A_t} e^{-ik_0 a} = \cos(ka). \quad (36)$$

This equation can be written differently. From Eqs.(31d) and (31e), one can check that $A_r A_t^* = i\alpha$ for real α , i.e.

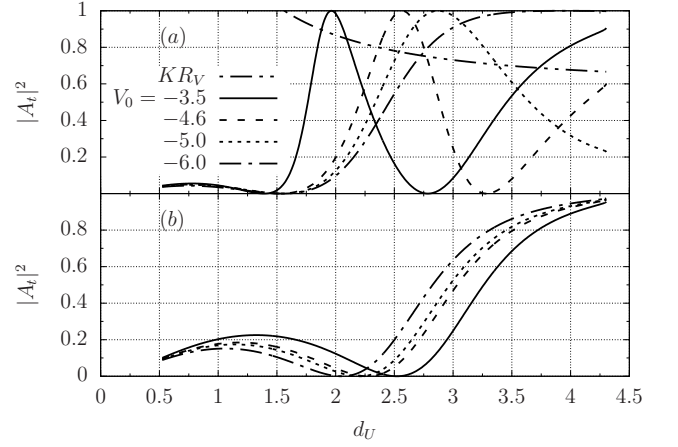


FIG. 1. Transmission coefficient $|A_t|^2$ as a function of the confinement length scale d_U (in units of R_V) for several values of the potential depth V_0 (in units of \hbar^2/mR_V^2), with $C \approx 2.58$ (square-well confinement U) and $k_0 R_V = 0.60$. The range $0.52 \approx 1/N_0 < d_U/R_V < C/k_0 R_V \approx 4.3$ follows from $R_V < R_U$ and Eq.(38b). (a) Both s - and p -waves are considered and one can see the CIRs for which $|A_t| = 0$ and also the dual CIRs for which $|A_t| = 1$. The curve at the top shows how small $K R_V$, given by $K^2 = q_0^2 + k_0^2$, is from unity (low energy condition). (b) Only the s -wave contribution is considered. Note that then $|A_t| \rightarrow 1$ only asymptotically.

this product is purely imaginary. Introducing the phase δ of A_t

$$A_t \equiv |A_t| e^{i\delta}, \quad (37)$$

it follows that $A_r = i\alpha e^{i\delta}/|A_t|$. Using $|A_r A_t^*| = |i\alpha|$ to extract $|A_t|$, one gets $A_r = i\alpha |A_r| e^{i\delta}/|\alpha|$. Taking this A_r and Eq.(37) into Eq.(36) and using Eq.(31f) gives thus

$$\frac{\cos(k_0 a + \delta)}{|A_t|} = \cos(ka), \quad (38a)$$

valid under the single channel constraint Eq.(11), which can be rewritten as

$$0 \leq k_0 d_U \leq C. \quad (38b)$$

Eq.(38a) is the desired equation that determines the energy band structure by giving k_0 or $E \equiv \hbar^2(q_0^2 + k_0^2)/2m$ as a function of the crystal momentum k . Not incidentally, this is nearly the same band structure equation as for the pure 1D case, for which $V(r)$ is replaced by a pure 1D potential $V_{1D}(z)$ (see e.g. Eq.(8.76), Chap.8, problem 1, p.148 in [1] or [30]).

The key difference, however, is that A_t here is critically dependent on the confinement, more specifically, on the parameter $d_U = R_U/N_0$ in the present case. The single channel constraint Eq.(11) implies the low energy condition $K \sim q_0 \sim 1/R_U \ll 1/R_V$, so that (see e.g. [39], §132)

$$K \cot \delta_0 \approx -1/a_s \quad \text{and} \quad K^3 \cot \delta_1 \approx -1/a_p^3, \quad (39a)$$

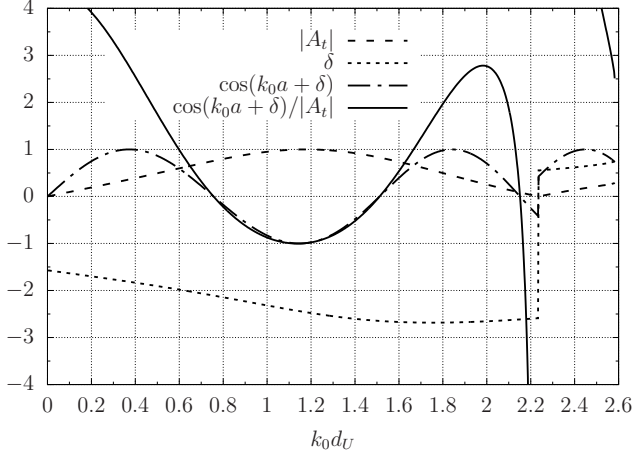


FIG. 2. An example of the elements of the lhs of Eq.(38a) as a function of the longitudinal energy $k_0 d_U$, whose range follows from Eq.(38b), using $C \approx 2.58$, $V_0 = -4.6\hbar^2/mR_V^2$, $a = 14.6R_V$ and $d_U = 3.00R_V$. Both s - and p -waves are included. One can see a zero gap for $k_0 d_U$ between 1 and 1.2 when an extremum of $\cos(k_0 a + \delta)$ coincides with a dual CIR $|A_t| = 1$. The discontinuity in δ (set to the interval $-\pi$ to π) stems from how A_t approaches and leaves the origin, for instance, from the third towards the first quadrant of the complex A_t plane.

where a_s and a_p are the so-called (three-dimensional) s - and p -wave scattering lengths. Energy-dependent corrections to Eq.(39a) may be accounted for but for simplicity we take a_s and a_p as constants. As a concrete example, we may assume V to be a spherical well of depth $V_0 < 0$ and radius R_V , so that one can calculate

$$a_s = \left(1 - \frac{\tan \xi}{\xi}\right) R_V, \quad (39b)$$

$$a_p^3 = \left(\frac{1}{3} - \frac{1 - \xi \cot \xi}{\xi^2}\right) R_V^3, \quad (39c)$$

where $\xi \equiv (-2mR_V^2 V_0/\hbar^2)^{1/2}$. For $|A_t| < 1$ in Eq.(38a), including the condition $|A_t| = 0$ called confinement induced resonance CIR [27–29], band gaps are expected to appear, whereas *zero gaps* would require the dual CIR condition $|A_t| = 1$, which is more suitable to appear when both s - and p -wave contributions are taken into account [32, 33]. The transmission coefficient $|A_t|^2$ is shown in Fig. 1 for (a) both s - and p -wave contributions and (b) only the s -wave contribution. An example of the influence of A_t is shown in Fig. 2, illustrating a typical behavior of the lhs of Eq.(38a) for which a zero gap is expected to appear.

When solving Eq.(38a), it is more convenient to vary k_0 and express k as a function of k_0 and then invert the relationship, which, however, results in few points for nearly flat bands. Using $C = 2.58$, $V_0 = -4.6\hbar^2/mR_V^2$ (such that both a_s and a_p are relatively large) and the lattice constant $a = 14.6R_V$, one can then obtain the bands for various values of d_U . This is done in Fig. 3, where

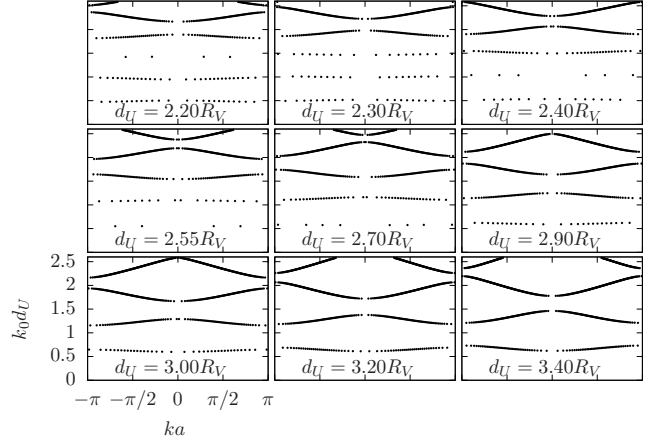


FIG. 3. Band structure for various values of the confinement length scale d_U when only the s -wave contribution is included. All graphs have the same axes. As expected, the bands do change under the influence of the confinement. However, closing a gap is hardly achieved.

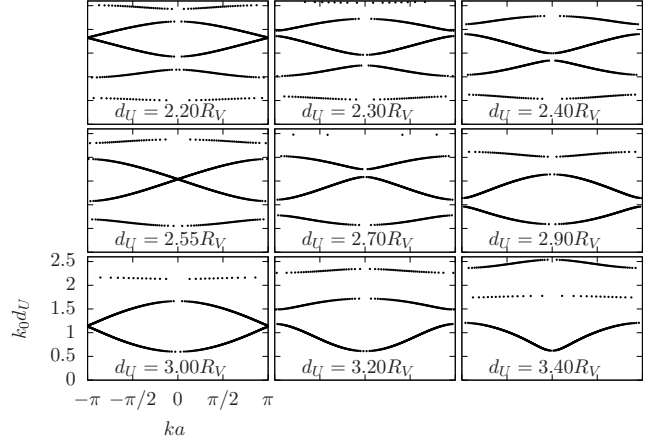


FIG. 4. The same as in Fig. 3, but including both the s - and p -waves. The difference here is that, besides more noticeable changes, zero gaps or nearly so do appear, either at the center or at the edges of the quasi-momentum k -space (first column of graphs), due to the appearance of dual CIRs $|A_t| = 1$.

the p -wave contribution is suppressed. In Fig. 4, on the other hand, it is kept for the sake of comparison and a practically zero gap can be observed, in addition to more pronounced changes to the bandwidths. Although beyond the scope of the present work, it may be noted that the first band shows a significant change as a function of d_U , which could be exploited for driving some parameters in a quasi-1D Bose-Hubbard Hamiltonian approximation as a function of the physical 3D parameters.

V. DISCUSSION

The possibility of opening and completely closing a band gap continuously as shown in Fig. 4 raises the prospect of dynamically driving a material between a (gap) insulator-like and a metal-like behavior if all other conditions are met such as the proper distribution of particles along the bands.

As trial systems, one may consider ionized impurities regularly placed along the axis of a semiconductor quantum wire surrounded by hard walls with different radii (see e.g. discussion at the end of Ref. [32] and references therein) or atom-ion systems as already suggested in [30] (see also [40]) for which trapped ions would form the lattice and the atom would move in an atom waveguide obtained, e.g., with an optical potential. An all optical system could also be tried.

Indeed, consider in more detail such optical potentials, which have the advantage of allowing to dynamically change the confinement in contrast to hard walls. The effective potential felt by a cold neutral atom, after time averaging over the fast optical oscillations, is proportional to the intensity of the laser field [2, 5]. Three pairs of counter-propagating laser beams with frequency ω_L and the same electric field amplitude E_L , with each pair along one of the three orthogonal axes and with suitable linear polarizations, can be made to yield the net electric field

$$2E_L[\sin(k_L x)\mathbf{e}_2 + \sin(k_L y)\mathbf{e}_3 + \sin(k_L z)\mathbf{e}_1] \cos(\omega_L t)$$

which, after time averaging over a period $T \approx 2\pi/\omega_L$, generates a 3D lattice potential

$$\tilde{V}_{latt}(\mathbf{r}) = V_L [\sin^2(k_L x) + \sin^2(k_L y) + \sin^2(k_L z)] \quad (40)$$

where V_L is proportional to $2E_L^2$. Adding then two other pairs of beams with frequency ω_C and amplitude E_C such as to provide the field (which alone would generate a

waveguide-like potential)

$$2E_C[\sin(k_C x)\mathbf{e}_2 + \sin(k_C y)\mathbf{e}_3] \cos(\omega_C t),$$

the total electric field of these five pairs of beams yields then the total optical potential

$$\begin{aligned} V_T(\mathbf{r}) = & \tilde{V}_{latt}(\mathbf{r}) \\ & + V_C \sin^2(k_C x) + 2\sqrt{V_L V_C} \sin(k_L x) \sin(k_C x) \\ & + V_C \sin^2(k_C y) + 2\sqrt{V_L V_C} \sin(k_L y) \sin(k_C y) \end{aligned} \quad (41)$$

where V_C is proportional to $2E_C^2$ and one assumes $\omega_C \approx \omega_L$, namely $|\omega_L - \omega_C| \ll \omega_L$. Close to the z -axis, one obtains approximately

$$V_T(\mathbf{r}) \approx \tilde{V}_{latt}(\mathbf{r}) + \tilde{U}(\rho) \quad (42)$$

where

$$\tilde{U}(\rho) \equiv \left(V_C k_C^2 + 2\sqrt{V_L V_C} k_L k_C \right) \rho^2 \quad (43)$$

would be the confining potential that could be tuned by varying the intensity V_C and the wavelength $\lambda_C = 2\pi/k_C$, provided the atoms could be carefully loaded close to the z -axis.

It must be noted that some assumptions made here may not be assured, particularly Eq.(2b) (although stretching the lattice spacing a may be attempted [9]) or the condition of simultaneously large contributions of s - and p -waves. However, if not all aspects of the present discussion, at least some of them, such as the continuous qualitative change the confinement may impose on the band structure, may then be illustrated.

ACKNOWLEDGMENTS

The author gratefully acknowledges fruitful discussions with Paulo A. Nussenzweig, Peter Schmelcher and Vladimir S. Melezhik and wish to thank Peter Schmelcher for reading an early version of the manuscript and for suggesting many improvements and references, particularly Ref. [30]. Financial support by the Universidade Federal de São Paulo is gratefully acknowledged.

-
- [1] N. W. Ashcroft and N. D. Mermin, *Solid State Physics* (Cengage Learning, New York, 1976).
 - [2] R. Grimm, M. Weidemüller, and Y. B. Ovchinnikov, Optical Dipole Traps for Neutral Atoms, in *Adv. At. Mol. Opt. Phys.*, Vol. 42 (Elsevier, 2000) pp. 95–170.
 - [3] I. Bloch, J. Dalibard, and W. Zwerger, Many-body physics with ultracold gases, *Rev. Mod. Phys.* **80**, 885 (2008).
 - [4] S. Giorgini, L. P. Pitaevskii, and S. Stringari, Theory of ultracold atomic Fermi gases, *Rev. Mod. Phys.* **80**, 1215 (2008).
 - [5] M. Lewenstein, A. Sanpera, and V. Ahufinger, *Ultracold*

Atoms in Optical Lattices: Simulating Quantum Many-Body Systems, 1st ed. (Oxford University Press, Oxford, U.K, 2012).

- [6] K. V. Krutitsky, Ultracold bosons with short-range interaction in regular optical lattices, *Phys. Rep.* **607**, 1 (2016).
- [7] S. Peil, J. V. Porto, B. L. Tolra, J. M. Obrecht, B. E. King, M. Subbotin, S. L. Rolston, and W. D. Phillips, Patterned loading of a Bose-Einstein condensate into an optical lattice, *Phys. Rev. A* **67**, 051603 (2003).
- [8] Z. Hadzibabic, S. Stock, B. Battelier, V. Bretin, and J. Dalibard, Interference of an Array of Independent

- Bose-Einstein Condensates, Phys. Rev. Lett. **93**, 180403 (2004).
- [9] L. Fallani, C. Fort, J. E. Lye, and M. Inguscio, Bose-Einstein condensate in an optical lattice with tunable spacing: Transport and static properties, Opt. Express **13**, 4303 (2005).
- [10] P. Jessen and I. Deutsch, Optical Lattices, in *Adv. At. Mol. Opt. Phys.*, Vol. 37 (Elsevier, 1996) pp. 95–138.
- [11] G. Grynberg and C. Robilliard, Cold atoms in dissipative optical lattices, Phys. Rep. **355**, 335 (2001).
- [12] W. H. Choi, P. G. Kang, K. D. Ryang, and H. W. Yeom, Band-Structure Engineering of Gold Atomic Wires on Silicon by Controlled Doping, Phys. Rev. Lett. **100**, 126801 (2008).
- [13] D. C. Elias, R. R. Nair, T. M. G. Mohiuddin, S. V. Morozov, P. Blake, M. P. Halsall, A. C. Ferrari, D. W. Boukhvalov, M. I. Katsnelson, A. K. Geim, and K. S. Novoselov, Control of Graphene's Properties by Reversible Hydrogenation: Evidence for Graphane, Science **323**, 610 (2009).
- [14] H. H. Pu, S. H. Rhim, C. J. Hirschmugl, M. Gajdardziska-Josifovska, M. Weinert, and J. H. Chen, Strain-induced band-gap engineering of graphene monoxide and its effect on graphene, Phys. Rev. B **87**, 085417 (2013).
- [15] O. Gülseren, T. Yildirim, S. Ciraci, and Ç. Kılıç, Reversible band-gap engineering in carbon nanotubes by radial deformation, Phys. Rev. B **65**, 155410 (2002).
- [16] H. Min, B. Sahu, S. K. Banerjee, and A. H. MacDonald, *Ab Initio* theory of gate induced gaps in graphene bilayers, Phys. Rev. B **75**, 155115 (2007).
- [17] E. V. Castro, K. S. Novoselov, S. V. Morozov, N. M. R. Peres, J. M. B. L. dos Santos, J. Nilsson, F. Guinea, A. K. Geim, and A. H. C. Neto, Biased Bilayer Graphene: Semiconductor with a Gap Tunable by the Electric Field Effect, Phys. Rev. Lett. **99**, 216802 (2007).
- [18] Y. Zhang, T.-T. Tang, C. Girit, Z. Hao, M. C. Martin, A. Zettl, M. F. Crommie, Y. R. Shen, and F. Wang, Direct observation of a widely tunable bandgap in bilayer graphene, Nature **459**, 820 (2009).
- [19] Y.-W. Son, M. L. Cohen, and S. G. Louie, Energy Gaps in Graphene Nanoribbons, Phys. Rev. Lett. **97**, 216803 (2006).
- [20] M. Y. Han, B. Özyilmaz, Y. Zhang, and P. Kim, Energy Band-Gap Engineering of Graphene Nanoribbons, Phys. Rev. Lett. **98**, 206805 (2007).
- [21] X. Li, X. Wang, L. Zhang, S. Lee, and H. Dai, Chemically Derived, Ultrasoft Graphene Nanoribbon Semiconductors, Science **319**, 1229 (2008).
- [22] E. Muñoz, Z. Barticevic, and M. Pacheco, Electronic spectrum of a two-dimensional quantum dot array in the presence of electric and magnetic fields in the Hall configuration, Phys. Rev. B **71**, 165301 (2005).
- [23] P. Drouvelis, G. Fagas, and P. Schmelcher, Magnetically controlled current flow in coupled-dot arrays, J. Phys.: Condens. Matter **19**, 326209 (2007).
- [24] C. Morfonios, D. Buchholz, and P. Schmelcher, Magneto-conductance switching in an array of oval quantum dots, Phys. Rev. B **80**, 035301 (2009).
- [25] T. Giamarchi, *Quantum Physics in One Dimension*, The International Series of Monographs on Physics No. 121 (Clarendon ; Oxford University Press, Oxford : New York, 2004).
- [26] V. A. Yurovsky, M. Olshanii, and D. S. Weiss, Collisions, correlations, and integrability in atom waveguides, in *Adv. At. Mol. Opt. Phys.*, Vol. 55 (Elsevier, 2008) pp. 61–138.
- [27] M. Olshanii, Atomic Scattering in the Presence of an External Confinement and a Gas of Impenetrable Bosons, Phys. Rev. Lett. **81**, 938 (1998).
- [28] V. Dunjko, M. G. Moore, T. Bergeman, and M. Olshanii, Confinement-Induced Resonances, in *Adv. At. Mol. Opt. Phys.*, Vol. 60 (Elsevier, 2011) pp. 461–510.
- [29] B. E. Granger and D. Blume, Tuning the Interactions of Spin-Polarized Fermions Using Quasi-One-Dimensional Confinement, Phys. Rev. Lett. **92**, 133202 (2004).
- [30] A. Negretti, R. Gerritsma, Z. Idziaszek, F. Schmidt-Kaler, and T. Calarco, Generalized Kronig-Penney model for ultracold atomic quantum systems, Phys. Rev. B **90**, 155426 (2014).
- [31] J. I. Kim, J. Schmiedmayer, and P. Schmelcher, Quantum scattering in quasi-one-dimensional cylindrical confinement, Phys. Rev. A **72**, 042711 (2005).
- [32] J. I. Kim, V. S. Melezhik, and P. Schmelcher, Suppression of Quantum Scattering in Strongly Confined Systems, Phys. Rev. Lett. **97**, 193203 (2006).
- [33] J. I. Kim, V. S. Melezhik, and P. Schmelcher, Quantum Confined Scattering beyond the s -Wave Approximation, Prog. Theor. Phys. Suppl. **166**, 159 (2007).
- [34] P. Giannakeas, F. K. Diakonos, and P. Schmelcher, Coupled l-wave confinement-induced resonances in cylindrically symmetric waveguides, Phys. Rev. A **86**, 042703 (2012).
- [35] B. Heß, P. Giannakeas, and P. Schmelcher, Energy-dependent l-wave confinement-induced resonances, Phys. Rev. A **89**, 052716 (2014).
- [36] B. Heß, P. Giannakeas, and P. Schmelcher, Analytical approach to atomic multichannel collisions in tight harmonic waveguides, Phys. Rev. A **92**, 022706 (2015).
- [37] V. S. Melezhik, J. I. Kim, and P. Schmelcher, Wavepacket dynamical analysis of ultracold scattering in cylindrical waveguides, Phys. Rev. A **76**, 053611 (2007).
- [38] P. M. Morse and H. Feshbach, *Methods of Theoretical Physics*, renewed ed. (Feshbach, Minneapolis, Minn, 1981).
- [39] L. D. Landau and E. M. Lifchitz, *Mécanique Quantique: Théorie Non Relativiste*, 3rd ed. (Éditions Mir, Moscou, 1980).
- [40] V. S. Melezhik and A. Negretti, Confinement-induced resonances in ultracold atom-ion systems, Phys. Rev. A **94**, 022704 (2016).